ACS APPLIED MATERIALS & INTERFACES

Research Article

www.acsami.org

Designed Synthesis of Aptamer-Immobilized Magnetic Mesoporous Silica/Au Nanocomposites for Highly Selective Enrichment and Detection of Insulin

Ya Xiong, Chunhui Deng,* Xiangmin Zhang, and Pengyuan Yang

Department of Chemistry and Institutes of Biomedical Sciences, Fudan University, 220 Handan Road, Shanghai 200433, China

Supporting Information

ABSTRACT: We designed and synthesized aptamer-immobilized magnetic mesoporous silica/Au nanocomposites (MMANs) for highly selective detection of unlabeled insulin in complex biological media using MALDI-TOF MS. The aptamer was easily anchored onto the gold nanoparticles in the mesochannels of MMANs with high capacity for highly efficient and specific enrichment of insulin. With the benefit from the size-exclusion effect of the mesoporous silica shell with a narrow pore size distribution (~2.9 nm), insulin could be selectively detected despite interference from seven untargeted proteins with different size dimensions. This method exhibited an excellent response for insulin in the range 2−1000 ng mL^{-1}. Moreover, good recoveries in the detection of insulin in 20-fold diluted human serum were achieved. We anticipate that this novel method could be extended to other biomarkers of interest and potentially applied in disease diagnostics.

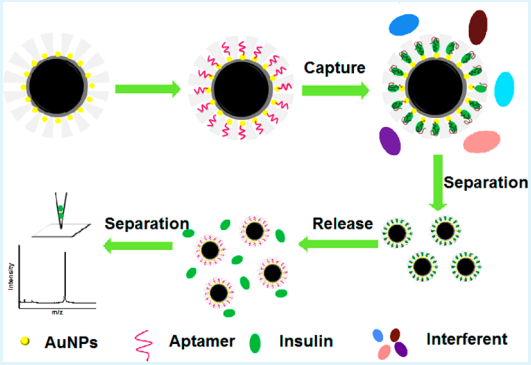

KEYWORDS: *insulin, magnetic mesoporous silica/Au nanocomposites, size-exclusion effect, aptamer, MALDI-TOF mass spectrometry*

INTRODUCTION

The insulin hormone plays a central role in physiological glycometabolism and is associated with diabetes and related diseases.[1−3] Highly sensitive and selective detection of this kind of disease biomarker in biological fluids is of profound value in clinical diagnostics, disease monitoring, and follow-up therapy.[4,5] Conventional immunoassays[6−11] are still standard technologies nowadays and are highly sensitive, but they generally require extremely tedious processes, expensive instruments, and qualified staffs. Currently, several innovative methods have been developed with great achievements as well as limitations. For instance, electrochemical antibody-based biosensors have been applied to the ultrasensitive detection of insulin in human blood.[12,13] However, they involve complicated and time-consuming electrode surface modification procedures, and the antibodies are expensive and unstable. Although new biomimetic receptors, as one of the alternatives to antibodies, have been synthesized for highly selective detection of insulin by taking advantage of the imprinting effect,[14] this method exhibits poor sensitivity. Aptamers have many inherent merits, apart from the specific binding affinity of the antibody, such as inexpensive synthesis, good stability, easy chemical modification, and no batch-to-batch variations.[15−17] Recently, the construction of nanomaterial-based aptasensors has offered new opportunities for improved performance of protein biomarker detection.[18,19] For example, aptamer-conjugated NIR fluorescent quantum-dots (QDs) have been designed to detect insulin with excellent sensitivity and selectivity.[20] However, it is worth noting that the QDs are toxic and unstable, and the weak $\pi-\pi$ stacking interaction between ssDNA and oxidized carbon nanoparticles (OCNPs) may lead to false positive results. Therefore, it is considerably demanding to develop a simple and robust method for both sensitive and selective detection of insulin in complex biological fluids.

Matrix-assisted laser desorption/ionization time-of-flight mass spectrometry (MALDI-TOF MS) has been extensively employed in detection of various disease biomarkers in biofluids with high sensitivity, accurate qualitative determination, fast speed, and high throughput.[21] In our previous work, aptamer-functionalized magnetic nanocomposites have dramatically contributed to target enrichment efficiency.[22,23] Nonetheless, the selective detection of a specific biomarker in the presence of excess interference was limited. As we know, insulin is present at low picomolar levels in human blood and is confronted with interference from a wide range of proteins and peptides as well as high levels of salts and lipids.[24−26] MS signals of less abundant insulin were normally suppressed by those of highly abundant species.[27,28] Thus, it is important to eliminate background interference as much as possible prior to MS analysis to improve detection selectivity.[29,30]

Mesoporous silica materials, because of their desirable features, are particularly accessible mesochannels with well-

Received: November 17, 2014
Accepted: April 9, 2015
Published: April 9, 2015

DOI: 10.1021/acsami.5b00515
ACS Appl. Mater. Interfaces 2015, 7, 8451−8456

designed pore size distribution, high surface area, hydrophilicity, and chemical stability, and have become attractive vehicles for highly selective capture of low molecular-weight targets (e.g., endogenous peptides,[31] phosphopeptides,[32] and N-glycans[33]) while excluding high molecular-weight targets by means of the size-exclusion mechanism.[34−36] Herein, for the first time, we synthesized aptamer-immobilized magnetic mesoporous silica/Au nanocomposites (MMANs) for insulin detection. As illustrated in Scheme 1, thiol group (SH) modified insulin binding aptamers (IBAs) are easily conjugated onto the surface of gold nanoparticles via the Au−S bond. The mesopores of obtained IBA-MMANs with suitable pore size allow insulin entrance while they repel large proteins outside of the mesochannels, serving as the "screening shell". Meanwhile, insulin is highly efficient and selectively enriched by numerous IBAs which fold into the compact G-quadruplex structure.[37] Thanks to the size-exclusion effect and magnetic separation, background interference is greatly diminished. Finally, the insulin-IBA-MMAN complex is exposed to a harsh environment to release the captured insulin. When incorporated with MALDI-TOF MS, our novel method enables fast analysis, accurate qualitative determination, and highly selective detection of insulin in complex media.

Scheme 1. Proposed Method for Insulin Detection Based on the IBA-MMAN Complex

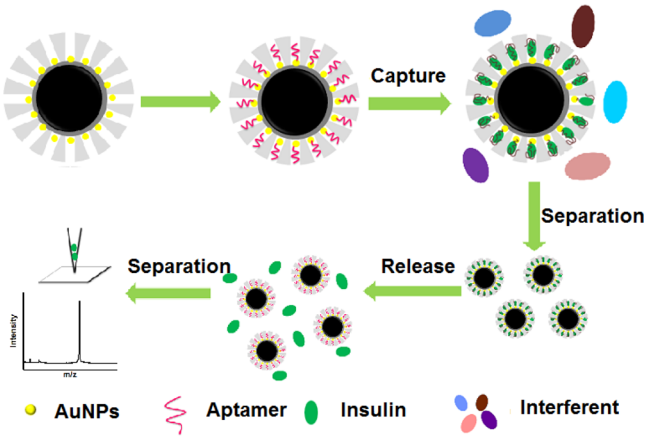

EXPERIMENTAL SECTION

Chemicals. The human insulin binding aptamers (IBAs) were synthesized by Sangon Biotechnology Company (Shanghai) with the following sequence: 5′-SH-$(CH_2)_6$-$(ACAG4TGTG4)_2$-3′. The human insulin, immunoglobulin G (IgG), human serum albumin (HSA), α_1-antitrypsin, horseradish peroxidase (HRP), β-casein, lysozyme, cytochrome C (Cyt C), trifluoroacetic acid (TFA), and α-cyano-4-hydroxycinnamic acid (CHCA) were purchased from Sigma-Aldrich. Tris(2-carboxyethyl) phosphine hydrochloride (TCEP) was obtained from Alfa Aesar. Other chemicals were all of analytical grade. Human serum was donated from Zhongshan Hospital (Shanghai). Ultrapure water (18.2 MΩ cm) was purified by a Milli-Q system (Millipore, Bedford, MA).

Synthesis of Magnetic Mesoporous Silica/Au Nanocomposites (MMANs). The MMANs were prepared using the protocol introduced by Deng et al. with slight modifications.[38] First, Fe_3O_4 particles were synthesized by our previous method.[39] Second, to obtain Fe_3O_4@SiO_2 particles with monodispersion and uniform thickness of silica, Fe_3O_4 particles (1.4 g) were first incubated with HCl aqueous solution (100 mL, 2 M), and then rinsed with deioned water. Then, the Fe_3O_4@SiO_2 particles were prepared via a sol−gel approach.[40] Third, the Fe_3O_4@SiO_2@Au composites were made with same method as described in the reported protocol. Finally, the Fe_3O_4@SiO_2@Au composites (0.16 g) were used as seeds, and mesoporous silica with controlled thickness was coated on the seeds via a CTAB-mediated sol−gel process. The other synthesis procedures stayed unchanged.

Characterizations. The morphologies of MMANs were investigated by transmission electron microscopy (JEOL 2011). Powder X-ray diffraction (XRD) patterns were recorded on a Bruker D4 X-ray diffractometer with Ni-filtered Cu Kα radiation (40 kV, 40 mA). Nitrogen sorption isotherms were measured at 77 K with a Micromeritcs Tristar 3000 analyzer. The Brunauer−Emmett−Teller (BET) surface area was obtained from the analysis of the adsorption isotherm in the relative pressure (P/P_0) range 0.036−0.28. Pore diameter and distribution curves were calculated by the BJH (Barrett−Joyner−Halenda) method from adsorption branch. The concentration of DNA was measured by a SHIMADZU UVmini-1240 spectrometer system at 260 nm. Magnetometry was examined using a superconducting quantum interference device (SQUID) at 300 K.

Preparation of IBA-MMANs. A 10 μM portion of IBAs was treated with 2.5 mM TCEP at pH 5.0 for 1 h in the dark. Afterward, MMANs were incubated with TCEP-activated IBAs for 12 h at room temperature in the dark. Subsequently, IBA-MMANs were separated from the supernatant with the help of a magnet. The collected IBA-MMANs were washed with 10 mM PBS (10 mM Na_2HPO_4, 2 mM KH_2PO_4, 137 mM NaCl, 2.7 mM KCl, pH 7.4) and stored in 10 mM TE buffer (10 mM Tris, 1 mM EDTA, pH 8.0) at 4 °C at a concentration of 20 mg mL^{-1} for further use. Then, absorption data for the supernatant containing unreacted IBA and the original IBA solution were determined by UV absorption spectrophotometer, respectively. The immobilization efficiency of IBA was calculated according to absorbency variation at 260 nm.

Enrichment of Insulin by IBA-MMANs. For insulin enrichment in standard solutions, 200 μL aliquots of insulin with different concentrations (2−5000 ng mL^{-1}) were equilibrated with 10 μL of IBA-MMAN suspension in PBS under vigorous shaking for 1 h. The insulin-IBA-MMAN material was isolated by magnetic separation and washed with PBS and 5% (v/v) acetonitrile (ACN) aqueous solution.

For the investigation of the size-exclusion effect of the as-prepared IBA-MMANs, insulin was mixed with seven proteins in PBS at a molar ratio of 1:50 (final concentrations: 34.4 nM insulin and 1.72 μM protein). Then, the mixture was incubated with IBA-MMANs for 1 h. The next steps were the same as those described above.

For real sample analysis, 20-fold diluted human serum samples were spiked with 500, 200, 100, 50, and 20 ng mL^{-1} insulin. Then, 200 μL portions of spiked samples were reacted with the IBA-MMANs for 1 h. The insulin-IBA-MMAN material was isolated by magnetic separation and washed with 10 mM PBS containing 0.1% Tween-20 to remove any nonspecific binding, and then rewashed with PBS to remove the residual Tween-20.

MALDI-TOF MS Analysis. A 1 μL portion of eluate was deposited onto the MALDI-MS plate, and then 3 μL of CHCA (4 mg/mL, 50% ACN, 0.1% TFA) was deposited as the matrix. MALDI mass spectra were obtained in linear positive ion mode using AB SCIEX TOF/TOF 5800 (Applied Biosystems) with the Nd:YAG laser at 355 nm, a repetition rate of 200 Hz, and an acceleration voltage of 20 kV.

RESULTS AND DISCUSSION

Characterization of MMANs. The as-fabricated multifunctional MMANs were characterized by several techniques. The Fe_3O_4 particles (a diameter of ∼300 nm) and Fe_3O_4@SiO_2 particles (a silica layer of ∼20 nm) are identified by the TEM images (Figure 1a,b). Wide-angle XRD patterns of Fe_3O_4@SiO_2@Au composites (Supporting Information Figure S1) demonstrate the efficient deposition of gold nanoparticles on the surface of Fe_3O_4@SiO_2 microspheres. As displayed in Figure 1c,d, the obtained MMANs are uniform and monodisperse with a mesoporous silica layer of ∼60 nm, and

DOI: 10.1021/acsami.5b00515
ACS Appl. Mater. Interfaces 2015, 7, 8451−8456

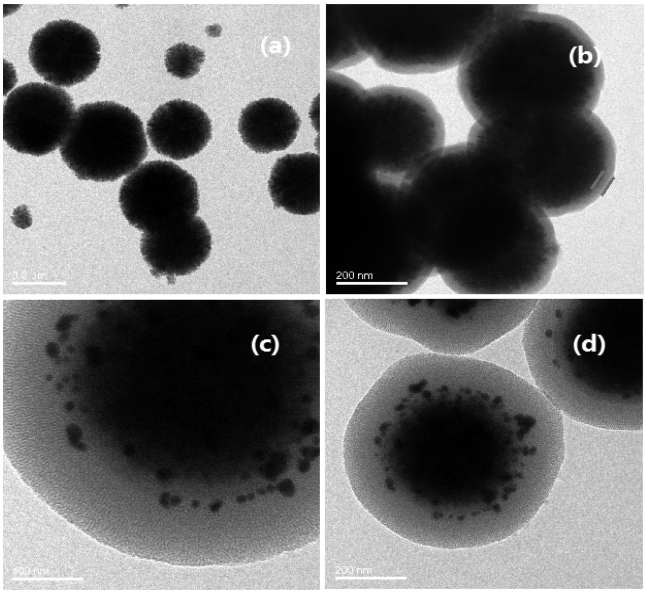

Figure 1. TEM images of (a) Fe_3O_4 particles, (b) Fe_3O_4@SiO_2 particles, and (c, d) MMANs.

tiny gold nanoparticles are densely embedded between the transparent mesoporous silica shell and the Fe_3O_4@SiO_2 core. The N_2 adsorption/desorption isotherm for MMANs (Figure 2a) exhibits a type IV isotherm with a BET surface area of 155 $m^2\ g^{-1}$ and a pore volume of 0.166 $cm^3\ g^{-1}$. The large surface area of MMANs allows the immobilization amount of IBA to be 0.246 nmol/mg (RSD = 8.13%, n = 6), which benefits recognition capability. The highly open mesochannels with a narrow pore size distribution at 2.9 nm are presented in Figure 2b, and are available for IBA and insulin (a mean value of 2.69 nm for an insulin monomer)[41] diffusion while excluding proteins with large size dimension via the size-exclusion effect. The magnetic hysteresis loop of the MMANs is indicated in Supporting Information Figure S2. The MMANs possess superparamagnetism, and the magnetization value is about 20.7 emu g^{-1}. Furthermore, the MMANs show a rapid response to the magnetic field and have good dispersibility in aqueous solution (Supporting Information Figure S3), which is crucial to enrichment and separation steps.

Investigation of Size-Exclusion Effect of IBA-MMANs. To investigate the size-exclusion effect of IBA-MMANs, insulin was mixed with several untargeted proteins with different dimensions with a 1:50 molar ratio of insulin to protein. The parameters of seven standard proteins are listed in Supporting Information Table S1. Before enrichment, insulin was difficult to distinguish, and only interferent peaks could be observed (Supporting Information Figure S4a–g). However, these peaks disappeared, and strong peaks assigned to insulin were shown after enrichment with IBA-MMANs (Figure 3a–g). Owing to the size-exclusion effect of the mesoporous silica shell, the untargeted proteins with size dimension larger than that of mesopores were excluded outside of the mesochannels while only insulin could enter, significantly eliminating background interference and resulting in high selectivity and enrichment efficiency. In contrast, a control experiment was carried out to verify the critical role of the mesoporous silica shell. IBA-conjugated Fe_3O_4@SiO_2@Au nanocomposites (IBA-MANs) were treated with the same complex samples. The MS intensity of insulin enriched by IBA-MANs was extremely low as a result

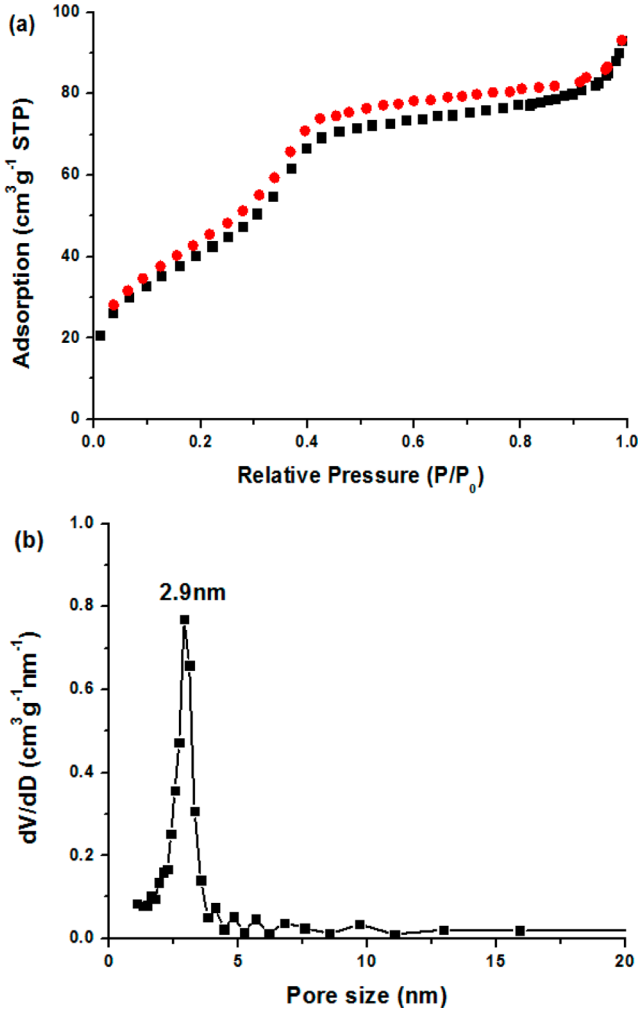

Figure 2. (a) Nitrogen adsorption–desorption isotherms and (b) pore size distribution of MMANs.

of suffering from serious interference and nonspecific competitive interaction of untargeted proteins with high concentrations (Supporting Information Figure S5a–g). All the results are in agreement with our expectation that the mesoporous silica shell can minimize the background signal and lead to enhanced selectivity and enrichment efficiency.

Determination of Insulin by IBA-MMANs. Several factors that could affect the release behaviors of insulin were studied (see details in the Supporting Information Figure S6). Under optimized conditions, the sensitivity of our method was estimated at various insulin concentrations, and the MS intensity increased with an increasing amount of insulin (Figure 4a). A good linear relationship with R^2 = 0.983 in the concentration range from 2 to 1000 ng mL^{-1} was obtained, as shown in Figure 4b. Saturation tendency occurred at higher concentrations (1000–5000 ng mL^{-1}, data not shown). Notably, the peak from insulin could still be identified when the concentration was as low as 2.0 ng mL^{-1} (0.344 nM) with signal-to-noise (S/N) ratio of 47.94 (Supporting Information Figure S7). This detection limit was much better than those of the previous methods using aptamer-based biosensors, 10 nM by Cha et al.[42] and 5 nM by Pu et al.[43] It validates the fact that both high capacity of aptamer and magnetism facilitate immunoreactions between the aptamer and the target, which improves detection sensitivity.

DOI: 10.1021/acsami.5b00515
ACS Appl. Mater. Interfaces 2015, 7, 8451–8456

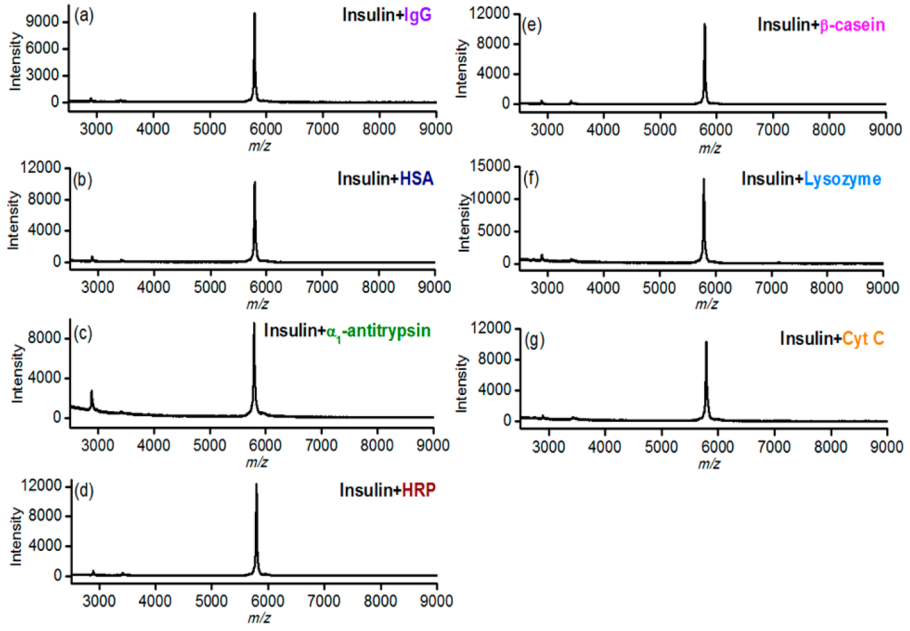

Figure 3. MALDI mass spectra (a–g) derived from a mixture of insulin and different proteins at molar ratio of 1:50 after enrichment by IBA-MMANs.

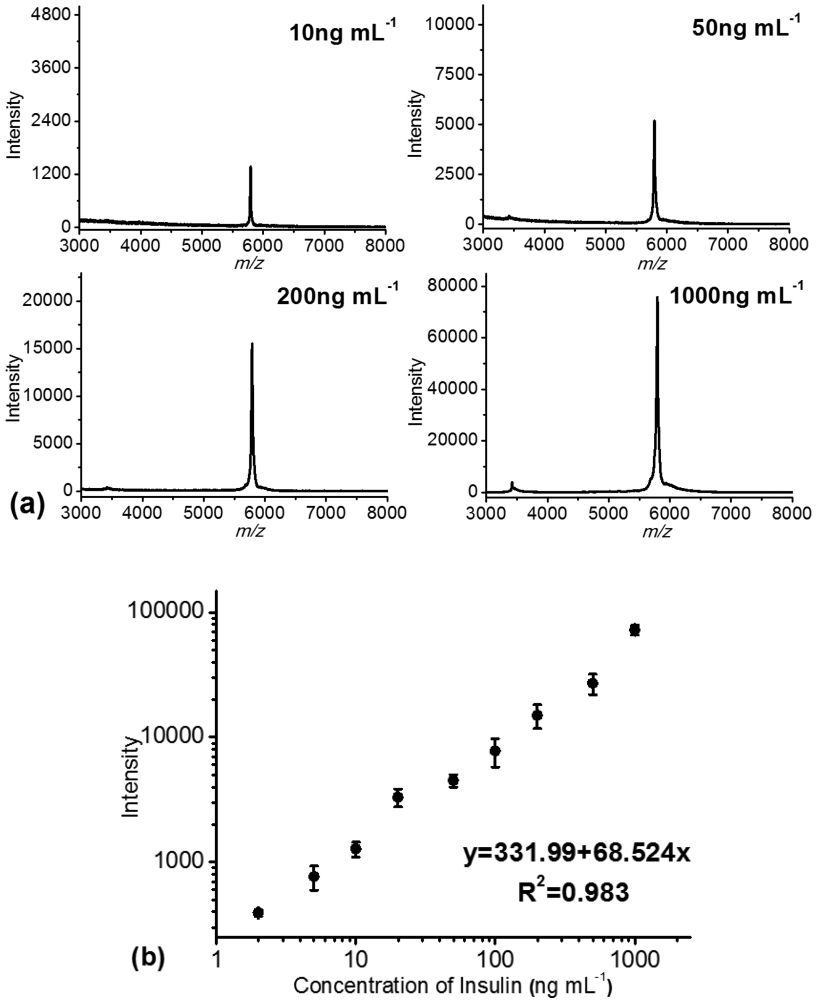

Figure 4. (a) Insulin detection in standard solutions in the range from 10 to 1000 ng mL^{-1}. The *S*/*N* ratios are 339.44, 948.73, 2236.33, and 5756.17, respectively. (b) Linear relationship between the MS intensity and the concentration of insulin. The error bars represent the standard deviation of three measurements.

DOI: 10.1021/acsami.5b00515
ACS Appl. Mater. Interfaces 2015, 7, 8451–8456

Application of IBA-MMANs for Insulin Determination in Human Serum. In order to examine the feasibility of our method for real sample analysis, we employed IBA-MMANs to determine insulin in 20-fold diluted human serum samples spiked with different amounts of insulin. Supporting Information Figure S8 describes the MS spectra of the samples with various concentrations from 500 to 20 ng mL^{-1} after enrichment with IBA-MMANs; the peaks of insulin (marked with asterisks) could be clearly identified. In addition, as displayed in Table 1, satisfactory recoveries of the four spiked serum samples were achieved.

Table 1. Insulin Detection in 20-Fold Diluted Human Serum Samples

sample no.	added (ng mL^{-1})	found (ng mL^{-1})	recovery (%)	RSD (%) $n = 3$
1	500	452.4	90.5	10.4
2	200	194.6	97.3	11.5
3	100	112.8	112.8	8.4
4	50	58.1	116.2	12.4

CONCLUSIONS

In summary, we have synthesized aptamer-immobilized magnetic mesoporous silica/Au nanocomposites (MMANs) for highly selective detection of unlabeled insulin using MALDI-TOF MS. Due to the large surface area and highly accessible mesoporous nature of MMANs, the aptamer is easily built in the mesochannels with high capacity. By combining the size-exclusion effect of mesopores with magnetism, the as-fabricated IBA-MMAN has been successfully utilized for highly selective and efficient enrichment of insulin from complex media. This reliable aptamer-based nanosystem coupled with MALDI-TOF MS holds new promise for other biomarker detection in biofluids.

ASSOCIATED CONTENT

Supporting Information

XRD patterns of Fe_3O_4 particles, Fe_3O_4@SiO_2 microspheres, and Fe_3O_4@SiO_2@Au composites; saturation magnetization curve of the MMANs; photos of MMAN aqueous dispersion; table containing the parameters of seven standard proteins; determination of the optimal release conditions and detailed discussion; additional MALDI-TOF MS spectra. This material is available free of charge via the Internet at http://pubs.acs.org.

AUTHOR INFORMATION

Corresponding Author

*Fax: +86-21-65641740. E-mail: chdeng@fudan.edu.cn.

Notes

The authors declare no competing financial interest.

ACKNOWLEDGMENTS

This work was supported by the 973 Project (2013CB911201, 2012CB910602), the 863 Project (2012AA020202), and the National Natural Science Foundation of China (21075022, 20875017, and 21105016).

REFERENCES

(1) Whiting, D. R.; Guariguata, L.; Weil, C.; Shaw, J. IDF Diabetes Atlas: Global Estimates of the Prevalence of Diabetes for 2011 and 2030. *Diabetes Res. Clin. Pract.* **2011**, *94*, 311−321.

(2) Van Belle, T. L.; Coppieters, K. T.; Von Herrath, M. G. Type 1 Diabetes: Etiology, Immunology, and Therapeutic Strategies. *Physiol. Rev.* **2011**, *91*, 79−118.

(3) Pierluissi, J.; Campbell, J. Metasomatotrophic Diabetes and Its Induction: Basal Insulin Secretion and Insulin Release Responses to Glucose, Glucagon, Arginine and Meals. *Diabetologia* **1980**, *18*, 223−228.

(4) Hermansen, K.; Fontaine, P.; Kukolja, K. K.; Peterkova, V.; Leth, G.; Gall, M. A. Insulin Analogues (Insulin Eetemir and Insulin Aspart) versus Traditional Human Insulins (NPH Insulin and Regular Human Insulin) in Basal-Bolus Therapy for Patients with Type 1 Diabetes. *Diabetologia* **2004**, *47*, 622−629.

(5) Carneiro, D. M.; Levi, J. U.; Irvin, G. L. Rapid Insulin Assay for Intraoperative Confirmation of Complete Resection of Insulinomas. *Surgery* **2002**, *132*, 937−942.

(6) Clark, P. M.; Levy, J. C.; Cox, L.; Burnett, M.; Turner, R. C.; Hales, C. N. Immunoradiometric Assay of Insulin, Intact Proinsulin and 32−33 Split Proinsulin and Radioimmunoassay of Insulin in Diet-Treated Type 2 (Non-Insulin-Dependent) Diabetic Subjects. *Diabetologia* **1992**, *35*, 469−474.

(7) Tanaka, T.; Matsunaga, T. Fully Automated Chemiluminescence Immunoassay of Insulin Using Antibody−Protein A−Bacterial Magnetic Particle Complexes. *Anal. Chem.* **2000**, *72*, 3518−3522.

(8) Even, M. S.; Sandusky, C. B.; Barnard, N. D.; Mistry, J.; Sinha, M. K. Development of A Novel ELISA for Human Insulin Using Monoclonal Antibodies Produced in Serum-Free Cell Culture Medium. *Clin. Biochem.* **2007**, *40*, 98−103.

(9) Thevis, M.; Thomas, A.; Delahaut, P.; Bosseloir, A.; Schänzer, W. Doping Control Analysis of Intact Rapid-Acting Insulin Analogues in Human Urine by Liquid Chromatography-Tandem Mass Spectrometry. *Anal. Chem.* **2006**, *78*, 1897−1903.

(10) Hess, C.; Thomas, A.; Thevis, M.; Stratmann, B.; Quester, W.; Tschoepe, D.; Madea, B.; Musshoff, F. Simultaneous Determination and Validated Quantification of Human Insulin and Its Synthetic Analogues in Human Blood Serum by Immunoaffinity Purification and Liquid Chromatography-Mass Spectrometry. *Anal. Bioanal. Chem.* **2012**, *404*, 1813−1822.

(11) Blachburn, M. Advances in the Quantitation of Therapeutic Insulin Analogues by LC−MS/MS. *Bioanalysis* **2013**, *5*, 2933−2946.

(12) Luo, X. L.; Xu, M. Y.; Freeman, C.; James, T.; Davis, J. J. Ultrasensitive Label Free Electrical Detection of Insulin in Neat Blood Serum. *Anal. Chem.* **2013**, *85*, 4129−4134.

(13) Luo, X. L.; Xu, Q.; James, T.; Davis, J. J. Redox and Label-Free Array Detection of Protein Markers in Human Serum. *Anal. Chem.* **2014**, *86*, 5553−5558.

(14) Schirhagl, R.; Latif, U.; Podlipna, D.; Blumenstock, H.; Dickert, F. L. Natural and Biomimetic Materials for the Detection of Insulin. *Anal. Chem.* **2012**, *84*, 3908−3913.

(15) Hermann, T.; Patel, D. J. Adaptive Recognition by Nucleic Acid Aptamers. *Science* **2000**, *287*, 820−825.

(16) Iliuk, A. B.; Hu, L. H.; Tao, W. A. Aptamer in Bioanalytical Applications. *Anal. Chem.* **2011**, *83*, 4440−4452.

(17) Mascini, M.; Palchetti, I.; Tombelli, S. Nucleic Acid and Peptide Aptamers: Fundamentals and Bioanalytical Aspects. *Angew. Chem., Int. Ed.* **2012**, *51*, 1316−1332.

(18) Yang, L.; Zhang, X. B.; Ye, M.; Jiang, J. H.; Yang, R. H.; Fu, T.; Chen, Y.; Wang, K. M.; Liu, C.; Tan, W. H. Aptamer-Conjugated Nanomaterials and Their Applications. *Adv. Drug Delivery Rev.* **2011**, *63*, 1361−1370.

(19) Kong, R. M.; Zhang, X. B.; Chen, Z.; Tan, W. H. Aptamer-Assembled Nanomaterials for Biosensing and Biomedical Applications. *Small* **2011**, *7*, 2428−2436.

(20) Wang, Y. H.; Gao, D. Y.; Zhang, P. F.; Gong, P.; Chen, C.; Gao, G. H.; Cai, L. T. A Near Infrared Fluorescence Resonance Energy Transfer Based Aptamer Biosensor for Insulin Detection in Human Plasma. *Chem. Commun.* **2014**, *50*, 811−813.

(21) Zhang, X.; Yuan, Z.; Shen, B.; Zhu, M.; Liu, C.; Xu, W. Discovery of Serum Protein Biomarkers in Rheumatoid Arthritis Using

DOI: 10.1021/acsami.5b00515
ACS Appl. Mater. Interfaces 2015, 7, 8451−8456

MALDI-TOF-MS Combined with Magnetic Beads. *Clin. Exp. Med.* **2012**, *12*, 145−151.
(22) Zhang, X. Y.; Zhu, S. C.; Deng, C. H.; Zhang, X. M. Highly Sensitive Thrombin Detection by Matrix Assisted Laser Desorption Ionization-Time of Flight Mass Spectrometry with Aptamer Functionalized Core−Shell Fe3O4@C@Au Magnetic Microspheres. *Talanta* **2012**, *88*, 295−320.
(23) Xiong, Y.; Deng, C. H.; Zhang, X. M. Development of Aptamer-Conjugated Magnetic Graphene/Gold Nanoparticle Hybrid Nanocomposites for Specific Enrichment and Rapid Analysis of Thrombin by MALDI-TOF MS. *Talanta* **2014**, *129*, 282−289.
(24) Iwase, H.; Kobayashi, M.; Nakajima, M.; Takatori, T. The Ratio of Insulin to C-Peptide Can Be Used To Make a Forensic Diagnosis of Exogenous Insulin Overdosage. *Forensic Sci. Int.* **2001**, *115*, 123−127.
(25) Ho, J. A. A.; Zeng, S. C.; Huang, M. R.; Kuo, H. Y. Development of Liposomal Immunosensor for the Measurement of Insulin with Femtomole Detection. *Anal. Chim. Acta* **2006**, *556*, 127−132.
(26) Zhang, X. Y.; Zhu, S. C.; Deng, C. H.; Zhang, X. M. An Aptamer Based On-Plate Microarray for High-Throughput Insulin Detection by MALDI-TOF MS. *Chem. Commun.* **2012**, *48*, 2689−2691.
(27) Qian, W. J.; Kaleta, D. T.; Petritis, B. O.; Jiang, H.; Liu, T.; Zhang, X.; Mottaz, H. M.; Varnum, S. M.; Camp, D. G.; Huang, L.; Fang, X.; Zhang, W. W.; Smith, R. D. Enhanced Eetection of Low Abundance Human Plasma Proteins Using aTandem IgY12-SuperMix Immunoaffinity Separation Strategy. *Mol. Cell. Proteomics* **2008**, *7*, 1963−1973.
(28) Qin, H.; Gao, P.; Wang, F.; Zhao, L.; Zhu, J.; Wang, A.; Zhang, T.; Wu, R. A.; Zou, H. Highly Efficient Extraction of Serum Peptides by Ordered Mesoporous Carbon. *Angew. Chem., Int. Ed.* **2011**, *50*, 12218−12221.
(29) Lee, S. J.; Adler, B.; Ekström, S.; Rezeli, M.; Vëgvári, Ä.; Park, J. W.; Malm, J.; Laurell, T. Aptamer/ISET-MS: A New Affinity-Based MALDI Technique for Improved Detection of Biomarkers. *Anal. Chem.* **2014**, *86*, 7627−7634.
(30) Rodthongkum, N.; Ramireddy, R.; Thayumanavan, S.; Richard, W. V. Selective Enrichment and Sensitive Detection of Peptide and Protein Biomarkers in Human Serum Using Polymeric Reverse Micelles and MALDI-MS. *Analyst* **2012**, *137*, 1024−1030.
(31) Liu, S. S.; Chen, H. M.; Lu, X. H.; Deng, C. H.; Zhang, X. M.; Yang, P. Y. Facile Synthesis of Copper(II) Immobilized on Magnetic Mesoporous Silica Microspheres for Selective Enrichment of Peptides for Mass Spectrometry Analysis. *Angew. Chem., Int. Ed.* **2010**, *49*, 7557−7561.
(32) Li, X. S.; Pan, Y. N.; Zhao, Y.; Yuan, B. F.; Guo, L.; Feng, Y. Q. Preparation of TItanium-Grafted Magnetic Mesoporous Silica for the Enrichment of Endogenous Serum Phosphopeptides. *J. Chromatogr. A* **2013**, *1315*, 61−69.
(33) Sun, N. R.; Deng, C. H.; Li, Y.; Zhang, X. M. Highly Selective Enrichment of N-Linked Glycan by Carbon-Functionalized Ordered Graphene/Mesoporous Silica Composites. *Anal. Chem.* **2014**, *86*, 2246−2250.
(34) Zhao, L.; Qin, H. Q.; Wu, R. A.; Zou, H. F. Recent Advances of Mesoporous Materials in Sample Preparation. *J. Chromatogr. A* **2012**, *1228*, 193−204.
(35) Zhu, C. L.; Wang, X. W.; Lin, Z. Z.; Xie, Z. H.; Wang, X. R. Cell Microenvironment Stimuli-Responsive Controlled-Release Delivery Systems Based on Mesoporous Silica Nanoparticles. *J. Food. Drug. Anal.* **2014**, *22*, 18−28.
(36) Tian, R. J.; Ren, L. B.; Ma, H. J.; Li, X.; Hu, L. H.; Ye, M. L.; Wu, R. A.; Tian, Z. J.; Liu, Z.; Zou, H. F. Selective Enrichment of Endogenous Peptides by Chemically Modified Porous Nanoparticles for Peptidome Analysis. *J. Chromatogr. A* **2009**, *1216*, 1270−1278.
(37) Connor, A. C.; Frederick, K. A.; Morgan, E. J.; McGown, L. B. Insulin Capture by an Insulin-Linked Polymorphic Region G-Quadruplex DNA Oligonucleotide. *J. Am. Chem. Soc.* **2006**, *128*, 4986−4991.
(38) Deng, Y. H.; Cai, Y.; Sun, Z. K.; Liu, J.; Liu, C.; Wei, J.; Li, W.; Liu, C.; Wang, Y.; Zhao, D. Y. Multifunctional Mesoporous Composite Microspheres with Well-Designed Nanostructure: A Highly Integrated Catalyst System. *J. Am. Chem. Soc.* **2010**, *132*, 8466−8473.
(39) Zhao, M.; Deng, C. H.; Zhang, X. M. The Design and Synthesis of a Hydrophilic Core−Shell−Shell Structured Magnetic Metal−Organic Framework as a Novel Immobilized Metal Ion Affinity Platform for Phosphoproteome Research. *Chem. Commun.* **2014**, *50*, 6228−6231.
(40) Xu, X.; Deng, C. H.; Gao, M. X.; Yu, W. J.; Yang, P. Y.; Zhang, X. M. Synthesis of Magnetic Microspheres with Immobilized Metal Ions for Enrichment and Direct Determination of Phosphopeptides by Matrix-Assisted Laser Desorption Ionization Mass Spectrometry. *Adv. Mater.* **2006**, *18*, 3289−3293.
(41) Oliva, A.; Fariña, J.; Llabrés, M. Development of two High-Performance Liquid Chromatographic Methods for the Analysis and Characterization of Insulin and Its Degradation Products in Pharmaceutical Preparations. *J. Chromatogr. B* **2000**, *749*, 25−34.
(42) Cha, T.; Baker, B. A.; Sauffer, M. D.; Salgado, J.; Jaroch, D.; Rickus, J. L.; Porterfield, D. M.; Choi, J. H. Optical Nanosensor Architecture for Cell-Signaling Molecules Using DNA Aptamer-Coated Carbon Nanotubes. *ACS Nano* **2011**, *5*, 4236−4244.
(43) Pu, Y.; Zhu, Z.; Han, D.; Liu, H. X.; Liu, J.; Liao, J.; Zhang, K. J.; Tan, W. H. Insulin-Binding Aptamer-Conjugated Graphene Oxide for Insulin Detection. *Analyst* **2011**, *136*, 4138−4140.

DOI: 10.1021/acsami.5b00515
ACS Appl. Mater. Interfaces 2015, 7, 8451−8456